

Structure and localisation of drug binding sites on neurotransmitter transporters

Aina W. Ravna · Ingebrigt Sylte · Svein G. Dahl

Received: 14 November 2008 / Accepted: 28 January 2009 / Published online: 24 February 2009
© Springer-Verlag 2009

Abstract The dopamine (DAT), serotonin (SERT) and noradrenalin (NET) transporters are molecular targets for different classes of psychotropic drugs. The crystal structure of *Aquifex aeolicus* LeuT_{Aa} was used as a template for molecular modeling of DAT, SERT and NET, and two putative drug binding sites (pocket 1 and 2) in each transporter were identified. Cocaine was docked into binding pocket 1 of DAT, corresponding to the leucine binding site in LeuT_{Aa}, which involved transmembrane helices (TMHs) 1, 3, 6 and 8. Clomipramine was docked into binding pocket 2 of DAT, involving TMHs 1, 3, 6, 10 and 11, and extracellular loops 4 and 6, corresponding to the clomipramine binding site in a crystal structure of a LeuT_{Aa}–clomipramine complex. The structures of the proposed cocaine- and tricyclic antidepressant-binding sites may be of particular interest for the design of novel DAT interacting ligands.

Keywords Neurotransmitter · Transporter protein · Binding site · Dopamine · Noradrenalin · Serotonin

Introduction

The dopamine transporter (DAT), serotonin transporter (SERT), and noradrenalin transporter (NET) are molecular targets for psychotropic drugs acting in the brain. DAT, SERT and NET regulate monoamine concentrations at neuronal synapses by carrying monoamines across neuronal

membranes into presynaptic nerve cells, using an inwardly directed sodium gradient as an energy source.

The dopaminergic system in the brain includes the mesolimbic-mesocortical pathway, which is involved in emotion- and drug-induced reward systems. This reward system, which is linked to drug abuse, is activated when a person receives positive reinforcement for certain behaviours, which can be both natural rewards and artificial rewards such as addictive drugs [1]. When stimulants such as cocaine bind to DAT, the dopamine concentration is elevated, resulting in a “reward”. Although the rewarding properties of cocaine are assumed to be due largely to its inhibition of DAT on terminals of mesolimbic-mesocortical dopaminergic neurons [2], SERT and NET inhibition also contribute to cocaine reward and cocaine aversion reactions [3, 4].

Both the serotonergic and noradrenergic neurons in the brain are associated with mood. Based on the observation that antidepressant drugs such as tricyclic antidepressants (TCA) and monoamine oxidase inhibitors (MAOI) facilitate monoaminergic transmission, the monoamine theory of depression, proposing that depression results from functionally deficient transmission of serotonin and noradrenalin in the central nervous system (CNS), was postulated in 1965 [5]. Although newer and more complex theories indicating that mood disorders are associated with impairment of structural plasticity in the CNS are currently replacing the monoamine theory of depression [6], the monoamine theory still remains a good basis for understanding the mechanism of action of antidepressant drugs. Modern antidepressants selectively inhibit serotonin- or noradrenalin-reuptake into presynaptic neurons. The class of antidepressant drugs termed selective serotonin reuptake inhibitors (SSRIs) elevates the concentration of serotonin at serotonergic synapses by binding to SERT, while selective noradrenalin

A. W. Ravna · I. Sylte · S. G. Dahl (✉)
Department of Pharmacology, Institute of Medical Biology,
Faculty of Medicine, University of Tromsø,
9037 Tromsø, Norway
e-mail: svein.dahl@uit.no

reuptake inhibitors (NARI) such as reboxetine elevate noradrenalin concentrations at noradrenergic synapses by binding to NET.

Structural information about DAT, SERT and NET transporters and their drug interactions is important for understanding their molecular mechanisms of action, and provide useful tools for new drug discovery. Cocaine and SSRIs share similar molecular mechanisms of action, although cocaine is a highly addictive drug and SSRIs are therapeutic drugs prescribed for the treatment of depression. Investigation of the molecular interactions of cocaine may aid in the development of compounds that block the binding of cocaine to DAT without inhibiting dopamine reuptake. Such compounds may have potential value in the treatment of cocaine addiction. Investigating the molecular interactions of SSRIs may be useful in the design of novel antidepressants with fewer side effects than existing ones.

Cocaine has similar binding affinities for DAT, SERT and NET, indicating that these transporters have a common core area for cocaine binding. Binding studies have demonstrated that SSRIs are from 300 to 3,500 times more selective for SERT over NET, and generally have low affinities for DAT [7]. Both cocaine and the SSRI S-citalopram block neurotransmitter reuptake competitively. However, while cocaine is a non-selective reuptake inhibitor, S-citalopram is a selective SERT inhibitor [8].

While no X-ray crystal structures of mammalian human DAT, SERT or NET have been reported, several molecular modelling studies on these transporters have been performed in the last decade [9–19]. A major advance in the monoamine transporter modelling field occurred in 2005 when the *Aquifex aeolicus* LeuT_{Aa} crystal structure, with leucine bound within the protein core, was published [20]. LeuT_{Aa} is a bacterial homologue of DAT, SERT and NET, and may be assumed to provide a valid template for molecular models of these transporters. The sequence identity between LeuT_{Aa} and monoamine transporters is ~20% [10]. In this study, we present models of DAT, SERT and NET based on the *Aquifex aeolicus* LeuT_{Aa} crystal structure. The electrostatic potential surfaces (EPS) were calculated, and two putative binding sites in each transporter have been identified. Cocaine and clomipramine were docked into the DAT model, and the results were compared with experimental data [21–33].

Computational methods

The SERT, DAT and NET models were constructed using the LeuT_{Aa} crystal structure (pdbcode 2a65) [20] as a template, and ICM software version 3.4-4 [34] was used for homology modelling. ICM performs homology modelling

by constructing the model from a few core sections defined by the average of C_α atom positions in the conserved regions. Loops are searched for by matching them with regard to sequence similarity and sterical interactions with the surroundings of the model, within several thousand high quality three dimensional (3D) protein structures. Maps around loops are calculated and the loops scored based on their relative energies, selecting the best fitting one. An amino acid sequence alignment [10] of all known prokaryotic and eukaryotic neurotransmitter:sodium symporter (NSS) proteins, including SERT, DAT and NET, based on the LeuT_{Aa} crystal structure, was used as input alignment in the ICM homology modelling module. The alignment used in the modelling procedure is shown in Fig. 1.

The RefineModel macro of ICM, including (1) a Monte Carlo simulation [34] of side chains, (2) five steps of iterative annealing of the backbone structure, and (3) a second Monte Carlo simulation of side chains, was used to globally optimise side-chain positions and anneal the backbones of the SERT, DAT and NET models. Step 1 performs a side-chain conformational analysis using the “MonteCarlo fast” option of the ICM global optimisation procedure for sampling of the conformational space of a molecule [35]. Random movements followed by local energy minimisations, then followed by a complete energy calculation, were performed iteratively. Each iteration was accepted or rejected based on energy and temperature criteria. In step 2, an iterative annealing of the backbone with provided tethers was performed. These tethers are harmonic restraints pulling an atom in the model to a static point in space represented by a corresponding atom in the template. In step 3, a second Monte Carlo side-chain sampling was performed.

The EPS of the SERT, DAT and NET models were calculated with the ICM program, with a potential scale from -10 to +10 kcal mol⁻¹. The stereochemical quality of the SERT, DAT and NET models were checked using the SAvs Metaserver for analysing and validating protein structures (<http://nihserver.mbi.ucla.edu/SAVS/>). Programs run were Procheck [36], What_check [37], and Errat [38], which examine the stereochemical quality of a protein structure by analysing its overall and residue-by-residue geometry.

ICMPocketFinder was used to explore possible drug binding pockets in the models, using a tolerance level of 4.6. Two putative binding sites were identified in each transporter, and, in DAT, cocaine and clomipramine were docked into binding pocket 1 and binding pocket 2, respectively, using the ICM program. Both ligands were first docked interactively into DAT, and poses in best agreement with experimental data were further examined by flexible docking. The resulting poses of cocaine were compared with site-directed mutagenesis data on DAT,

Fig. 1 Input alignment for the ICM homology modelling procedure. Alpha helices in the LeutAa X-ray crystal structure are displayed as *black cylinders*, and beta-sheets in the LeutAa X-ray crystal structure are displayed as *grey arrows*

LeuT_Xray	1	-----
Human_DAT	1	-----MSKSKCSVGLMSSVVAPAKEPNAVGPKVEVELILVKEQNGVQ
Human_NET	1	-----MLLARMNPQVQPEENNGADTGPEQPLRARKTABELLVVK
Human_SERT	1	METTPLNSQKQLSACEDGEDCQENGVLQKVVPPTPGDKVESGQISNGYSAVPSPGAGDDTR
LeuT_Xray		-----
LeuT_Xray	1	-----REHWATRLGLILAMAGNAVGLGNFLRFVQAAENGGGAFMIF
Human_DAT	42	LTSSTLTNPRQSPVEAQDRETWGKKIDFLLSVIGFAVDLANVWRFPYLCYKNGGGAFLLVP
Human_NET	38	ERNGVQCLLAPRDGDAQPRETWGKKIDFLLSVVGFVAVDLANVWRFPYLCYKNGGGAFLLIP
Human_SERT	61	HSIPATTTTLVAELHQGERETWGKKVDFLLSVIGYAVDLGNVWRFPYICYQNGGGAFLLP
LeuT_Xray		-----
LeuT_Xray	43	YIIAFLLVGIPLMWIEWAMGRYGAQGHGTTPAIFYLLWRNRFKILGVFLWIPLVVAI
Human_DAT	102	YLLFMVIAGMPLFYMELALGQFNREGAAGVWK-ICP-----ILKGVGFTVILISLYVGF
Human_NET	98	YTLFLIIAGMPLFYMELALGQYNREGAATVWK-ICP-----FFKGVGYAVILIALYVGF
Human_SERT	121	YTIMAIFFGGIPLFYMELALGQYHRNGCISIWKIKCP-----IFKIGIYAICIIAFYIAS
LeuT_Xray		-----
LeuT_Xray	103	YYVYIESWTLGFAIKFLVGLVEPPP--T-----DPDSILRPF
Human_DAT	155	FYNVIIAALHLYLFSSTTELPWIHCNNSWNSPNCSDAHPGD-SSGDSSGLNDTFGTTTPA
Human_NET	151	YYNVIIAWSLYLFSSTTLNLPWTDGCHTWNPNCTDPKLLNGSVLGNHTKYSKYKFTPA
Human_SERT	175	YYNTIMAWALYYLISSTFDQLPWTSCKNWNTGNTNYFSED-----NITWTLHSTSPA
LeuT_Xray		-----
LeuT_Xray	139	KEFLYSYIGVPGK--DEPILKPSLFAYIVFLITMFINVSIILIRGISKGIERFAKIAMP
Human_DAT	214	AEYFERGVLHLHQSHGIDDLGPPRWQLTACLVLVIVLLYFSLWKGVKT-SGKVVWITATM
Human_NET	211	AEFYERGVHLHESGGIHDIGLPQWQLLCLMVVVIVLYFSLWKGVKT-SGKVVWITATL
Human_SERT	229	EEFYTRHVLQIHRSKGLQDLGGISWQLALCIMLIFTVIYFISWKGVKT-SGKVVWVWATP
LeuT_Xray		-----
LeuT_Xray	196	LFILAVFLVIRVFLLETPNGTAADGLNFWLWTPDFEKLKDPGVWIAAVGQIFFTLSLGFGA
Human_DAT	273	PYVVLTAALLRGVTLP---GAIDGIRAYLSVDFYRLCEASVWIDAATQVCFSLGVGFVG
Human_NET	270	PYFVLFVLLVHGVTLP---GASNGINAYLHDFYRLKEATVWIDAATQIFFSLGGAGFV
Human_SERT	288	PYIILSVLLVRGATLP---GAWRGVLFYLPKNWQKILETVWIDAAAQIFFSLGPFGV
LeuT_Xray		-----
LeuT_Xray	256	IITYASYVRKQDIVLSGLTAATLNEKAEVILGGSISIPAAVAFVGVANAVATAKAG---
Human_DAT	329	LIAFSSYNKFTNNCYRDAIVTTSINSLTSFSSGFVVFSLGYMA--QKHSVPIGDVAKD-
Human_NET	326	LIAFASYNKFDNNCYRDALLTSSINCITSFVSGFAIFSLGYMA--HEHKVNIEDVATE-
Human_SERT	344	LLAFASYNKFNNNCYQDALVTSVNNCMTSFVSGFVIPTVLGYMA--EMRNEDEVSEVAKDA
LeuT_Xray		-----
LeuT_Xray	313	AFNLGFTITLPAIFSQTAGGTFLGLFWFLFFAGLTSIIAQMPIAFLEDELKLDKLDK---
Human_DAT	386	GPGLIFIIYPEAIATLPLSSAWAVVFFIMLLTLGIDSAMGGMESVITGLIDEFQLLHR-H
Human_NET	383	GAGLVFIIYPEAISTLSGSTFWAVVFFVMLLALGLDSSMGMEAVITGLADDFQVLKR-H
Human_SERT	402	GPSLLFITYAEAIANMPASTFFAIIFFLMLITLGLDSTFAGLEGVITAVLDEFPHVWAKR
LeuT_Xray		-----
LeuT_Xray	369	RKHAVLWTAIVFFSAHLVMFL--NKSLEDMDFWAGTIGVVFVGLTELIIFFWIFGADKA
Human_DAT	445	RELFTLFIVLATFLLSLFCVNTGGIYVFTLLDHFAAGTSLIFGVLEAIGVAVFYGVGQF
Human_NET	442	RKLFTFGVTFSTFLALFCITKGGIYVFTLLDTFAAGTSLIFAVLMEAIGVSWFYGVDRF
Human_SERT	462	RERFVLAVVITCFFGSLVTLTFGGAYVKLLEEYATGPAVLTVALLIEAVAVSWFYGITQF
LeuT_Xray		-----
LeuT_Xray	427	WEEINRGGIIKVPRIYYVMRYITPAFLAVLLVWAREYIPKIMEETH---WTVWITRFY
Human_DAT	505	SDDIQQMTGQRPSLYWRLCWKLVSPCFLFVVVVSVIVTFRPPHYGAYIFPDWANALGWVI
Human_NET	502	SNDIQQMMGFRPGLYWRLCWKFVSPAFLLFVVVVSIIINFKPLTYDDYIFPPWANVWGVI
Human_SERT	522	CRDVKEMLGFSPGWFWRICWVAISPLFLFLFIICSFLMSPQRLRFQYNYPPYWSIILGYCI
LeuT_Xray		-----
LeuT_Xray	484	IIGLFLFLTFLVFLAERRRNHESAGT-----
Human_DAT	565	ATSSMAMVPIYAAKFCSLPGSFREKLAYAIAPKDRLELVDRGEVRQFTLRHWLKV---
Human_NET	562	ALSSMVLVPIYVIYKFLSTQGSWLERLAYGITPENEHHLVAQRDIRQFQLQHWLAI---
Human_SERT	582	GTSSFICIPTYIAYRLIITPGTFKERIKSITPETPTEIPC-GDIRLNAV-----
LeuT_Xray		-----

which indicated that Asp79 is involved in ligand binding [24] by forming a salt-bridge with the positively charged nitrogen atom on cocaine, and-site directed mutagenesis studies on DAT [28] and SERT [26], which suggested other amino acids involved in ligand binding. Poses from the docking of clomipramine were compared with an X-ray crystal structure of LeuT_{Aa} with clomipramine bound in the extracellular-facing cavity [32].

Coordinates are available from the authors upon request.

Results

The DAT, SERT and NET models with their water-accessible surfaces and putative drug binding pockets, colour coded according to their EPS, are shown in Figs. 2, 3 and 4.

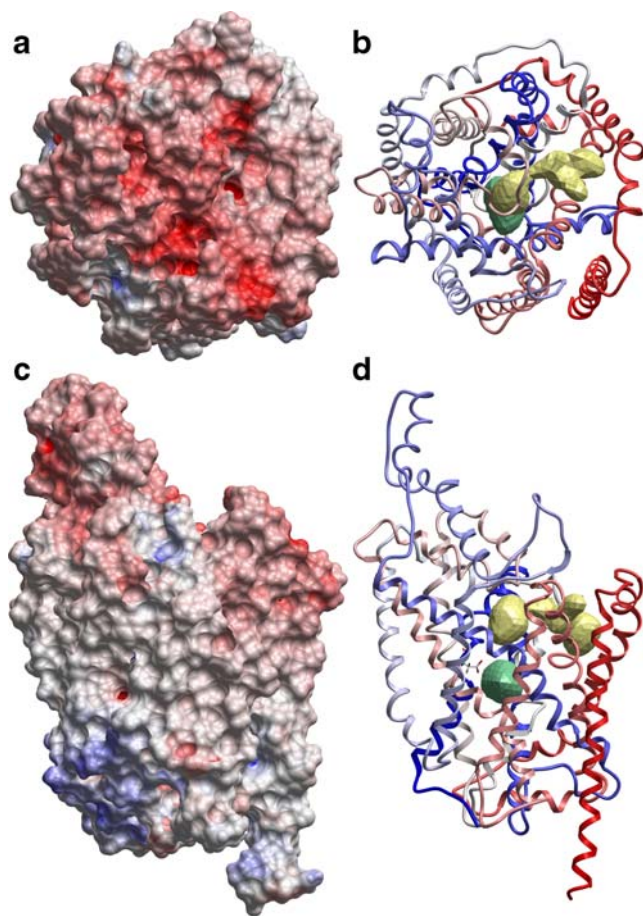


Fig. 2 Dopamine transporter (DAT) model, viewed from the extracellular side (**a**, **b**), and in the membrane plane with the extracellular side up (**c**, **d**). The water-accessible surface (**a**, **c**) is colour coded according to the electrostatic potentials 1.4 Å outside the surface. Scale: *Red* Negative ($-10 \text{ kcal mol}^{-1}$), to *blue* positive ($+10 \text{ kcal mol}^{-1}$). Binding pocket 1 is displayed in *green*, and binding pocket 2 is displayed in *yellow*. Colouring of the C α traces of the model is *blue* via *white* to *red* from N-terminal to C-terminal

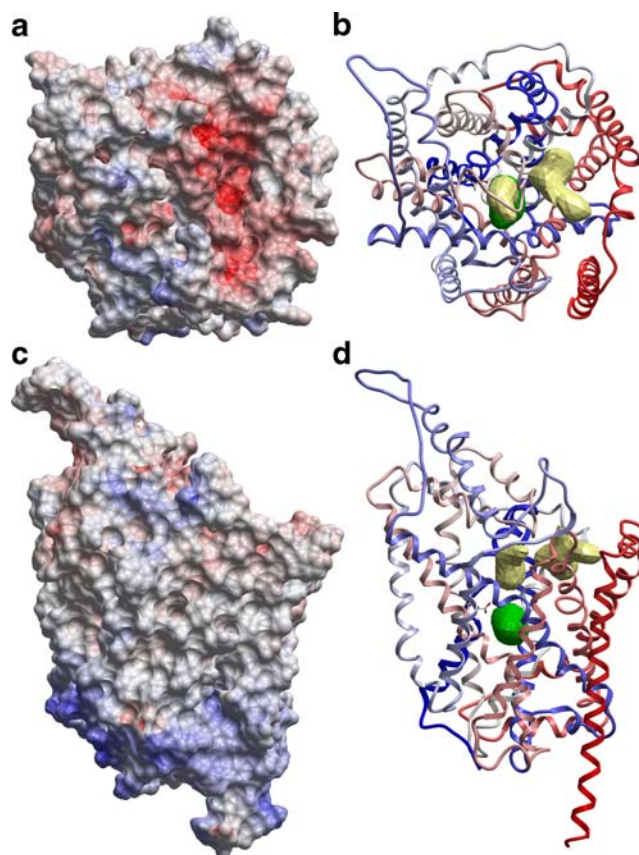


Fig. 3 Serotonin transporter (SERT) model, viewed from the extracellular side (**a**, **b**), and in the membrane plane with the extracellular side up (**c**, **d**). Colour coding as in Fig. 2

In each model, TMH 1-5 and 6-10 were arranged with a pseudo-twofold axis in the membrane plane, constituting the protein core of the 12 TMH bundle. As in the LeuT_{Aa} crystal structure [20], the DAT, SERT and NET models resembled shallow ‘shot glasses’, with a tight opening towards the extracellular side. TMH6 was kinked near the drug binding site.

Viewed from the extracellular side (Figs. 2a, 3a, 4a), the EPS of the entrance of the substrate permeation pathway of each of the DAT, SERT and NET models was distinctly more negative than other areas. The EPS of the models, viewed in the membrane plane (Figs. 2c, 3c, 4c), show that each transporter model has a dipole moment, being more negative towards the extracellular side. This is in accordance with the general ‘positive inside rule’ for membrane proteins [39].

For each model, ICMPocketFinder identified two putative drug-binding pockets, one (binding pocket 1) located halfway across the membrane bilayer in the area corresponding to the substrate binding pocket of leucine in the LeuT_{Aa} crystal structure [20], and one (binding pocket 2) in the extracellular-facing cavity forming part of the substrate permeation pathway, as shown in Figs. 2(b,d), 3(b,d) and 4(b,d). Amino acids in TMHs 1, 3, 6 and

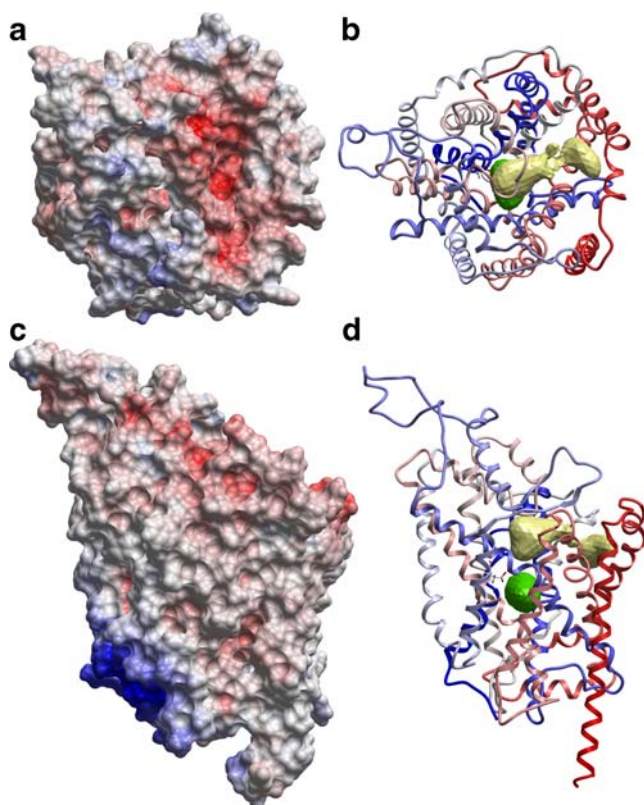


Fig. 4 Noradrenalin transporter (NET) model, viewed from the extracellular side (**a**, **b**) and in the membrane plane with the extracellular side up (**c**, **d**). Colour coding as in Fig. 2

Table 1 Amino acids in binding pocket 1 (ICM Pocket Finder) of the dopamine transporter (DAT), serotonin transporter (SERT), and noradrenalin transporter (NET). *TMH* Trans-membrane helix

	DAT	NET	SERT
TMH1	Phe76 Ala77 Asp79 Ala81	Phe72 Ala73 Asp75 Ala77	Tyr95 ^a Ala96 Asp98 Gly100 ^a
TMH3	Ser149 ^a Val152 Gly153 Tyr156	Ala145 Val148 Gly149 Tyr152	Ala169 Ile172 ^a Ala173 ^a Tyr176
TMH6	Phe320 Ser321 Gly323 Phe326 Val328	Phe317 Ser318 Gly320 Phe323 Val325	Phe335 Ser336 Gly338 Phe341 Val343
TMH8	Ser422 Ala423 ^a Gly425 Gly426	Ser419 Ser420 ^a Gly422 Gly423	Ser438 Thr439 ^a Ala441 ^a Gly442

^aNon-conserved amino acids

8 contributed to binding pocket 1 (Table 1), while amino acids in TMHs 1, 3, 6, 10 and 11, as well as in the extracellular loops between TMH7 and TMH8 (EL4), and TMH11 and TMH12 (EL6), contributed to binding pocket 2 (Table 2).

The stereochemical qualities of the DAT, SERT and NET models, analysed with the Procheck [36], What_Check [37], and Errat [38] procedures, are shown in Table 3. The overall quality factors were in the range of 87.5–89.7, indicating a valid stereochemistry of the models.

Figure 5 shows a close-up of the two binding pockets in DAT displaying their hydrophobic and hydrophilic properties.

Table 2 Amino acids in binding pocket 2 (ICM Pocket Finder) of DAT, NET and SERT

	DAT	NET	SERT
TMH1	Leu80 Ala81 Trp84 Arg85 Tyr88 Leu89	Leu76 Ala77 Trp80 Arg81 Tyr84 Leu85	Leu99 Gly100 ^a Trp103 Arg104 Tyr107 Ile108 ^a
TMH3	Phe155 ^a Tyr156 Ile159 Trp162	Tyr151 Tyr152 Ile155 Trp158	Tyr175 Tyr176 Ile179 Trp182
TMH6	Ile312 Asp313 Thr316 Phe320	Ile309 Asp310 Thr313 Phe317	Ile327 Asp328 Ala331 ^a Phe335
EL4	Lys384 Asp385 (Gap) Gly386 Pro387	Thr381 ^a Glu382 ^a (Gap) Gly383 Ala384 ^a	Lys399 Asp400 Ala401 ^a Gly402 Pro403
TMH10	Phe472 ^a Thr473 Asp476 His477 ^a Ala480 Gly481 Thr482 Leu485	Leu469 ^a Thr470 Asp473 Thr474 ^a Ala477 Gly478 Thr479 Leu482	Val489 ^a Lys490 ^a Glu493 ^a Glu494 ^a Thr497 ^a Gly498 Pro499 ^a Leu502
TMH11	Ser539 Phe543 Arg544 ^a	Ser536 Phe540 Lys541 ^a	Phe556 ^a Pro560 ^a Pro561 ^a
EL6	His547 ^a Tyr548 Tyr551	Thr544 ^a Tyr545 Tyr548	Arg564 ^a Leu565 ^a Tyr568

^aNon-conserved amino acids

Table 3 Validation of transporter protein structures

	PROCHECK (Ramachandran Plot)				WHAT_CHECK	ERRAT
	Core ^a (%)	Allow ^b (%)	Gener ^c (%)	Disall ^d (%)		
SERT	94.0	6.0	0.0	0.0	Satisfactory	87.7
DAT	94.2	5.8	0.0	0.0	Satisfactory	87.5
NET	93.8	6.0	0.0	0.0	Satisfactory	89.7

^a Most favoured regions^b Additional allowed regions^c Generously allowed regions^d Disallowed regions (<http://nihserver.mbi.ucla.edu/SAVS/>)

Binding pocket 1 featured both hydrophobic and hydrogen bond acceptor properties, while binding pocket 2 featured hydrophobic and slightly hydrogen bond donor properties. The hydrogen acceptor properties in binding pocket 1 were centred around Asp79 (TMH1), while Arg85 (TMH1) contributed to the hydrogen bond donor properties in binding pocket 2.

Figure 6 shows a cocaine pose after docking the cocaine molecule in flexible DAT. The figure illustrates the interaction of cocaine with amino acids reported to be part of a cocaine-binding site in site-directed mutagenesis studies: Asp79

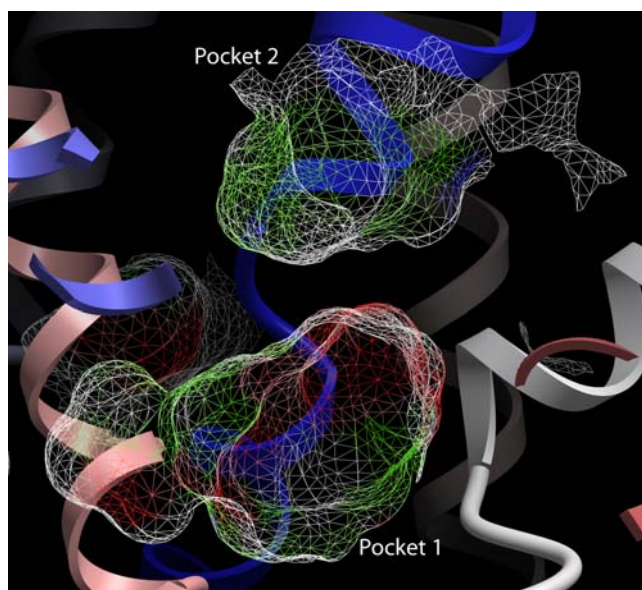


Fig. 5 Close-up of the two binding pockets in DAT viewed in the membrane plane (cytoplasm downwards) displaying their hydrophobic and hydrophilic properties. *Green areas* Hydrophobic properties, *red areas* hydrogen bond acceptor properties, *blue areas* hydrogen bond donor properties. Colouring of the C α traces of the model is *blue* via *white* to *red* from N-terminal to C-terminal

(TMH1) [24], Val152 (TMH3) [28], and Tyr156 (Tyr176 in SERT) (TMH3) [26]. The docking indicated a salt-bridge between Asp79 and the positively charged nitrogen atom of cocaine, and that aromatic interactions may be formed between Tyr156 and the aromatic ring of cocaine. Other interactions observed in the cocaine-DAT complex were cation- π interactions between Phe76 (TMH1) and the positively charged nitrogen atom of cocaine, aromatic interactions between Phe320 (TMH6) and the aromatic ring of cocaine, and hydrophobic interactions between Phe326 (TMH6) and the tropane ring of cocaine.

A clomipramine pose after docking the clomipramine molecule in flexible DAT is shown in Fig. 7. The crystal structure of a LeuT_{Aa}-clomipramine complex [32] was superimposed with the DAT-clomipramine complex, and clomipramine from the LeuT_{Aa}-clomipramine complex [32] is displayed for comparison with the clomipramine pose after flexible docking. The orientations of the docked clomipramine molecule and the clomipramine molecule superimposed from the crystal structure are similar; the tricyclic moieties almost overlap, and the side-chains are orientated in the same direction. However, compared with LeuT_{Aa}, DAT has an insertion in EL4 (Lys384 and Asp385) (Fig. 1) and, after docking, the side-chain of clomipramine had moved away from Lys384 because of sterical hindrance. In the complex of clomipramine docked into flexible DAT, a salt-bridge may be formed between the positively charged nitrogen atom of clomipramine and Asp385, and possibly also with Asp476 (TMH10). The chloride atom connected to the tricyclic moiety of clomipramine was situated between Arg85 (TMH1) and Lys384. Aromatic interactions were observed between the aromatic rings of clomipramine and Tyr156 (TMH3), and Phe320 (TMH6). Phe155 (TMH3) was oriented towards the nitrogen atom in the tricyclic moiety of clomipramine.

Discussion

Structural studies of drug interactions with different molecular targets have made significant contributions to drug discovery and the understanding of the molecular mechanisms of drug action. In particular, molecular modelling may be used to investigate the intermolecular forces determining the potency and specificity of drug action on a target. DAT, SERT and NET are membrane proteins, for which crystallisation is technically difficult. Molecular modelling based on homology with a known crystal structure may therefore provide valuable insights into their structure and molecular mechanisms. Homology between two proteins may be determined by sequence similarity, indicating the presence of similar features such

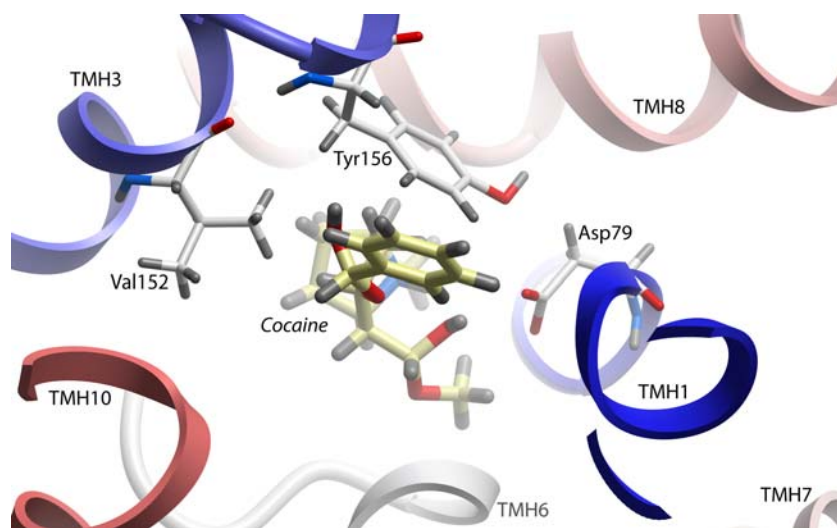


Fig. 6 Cocaine in DAT binding pocket 1 after interactive docking and subsequent docking in flexible DAT, viewed from the extracellular side. Amino acids reported to be part of a cocaine-binding site in site-directed mutagenesis studies: Asp79 [trans-membrane helix (TMH)1]

[24], Val152 (TMH3) [28], and Tyr156 (Tyr176 in SERT) (TMH3) [26] are displayed as *sticks*. Colour coding: *Red* O, *blue* N, *grey* H, *yellow* C in cocaine, *white* C in DAT. Colouring of the C α traces of the model is *blue* via *white* to *red* from N-terminal to C-terminal

as homologous protein folds. The transport mechanism of LeuT_{Aa} uses an electrochemical sodium gradient to provide an inward movement of substrate against a concentration gradient, and thus resembles the transport mechanisms of DAT, SERT and NET. Their related functional mechanisms and amino acid sequence indicate that these proteins share a common overall folding of their membrane spanning regions, and that the LeuT_{Aa} crystal structure may serve

as a suitable template for homology modeling of DAT, SERT and NET.

In order to obtain a valid molecular model of a protein using a crystal structure of another protein as template, the target–template amino acid alignment should be optimal, and it should be possible to identify corresponding positions in the target and the template. We have previously constructed a SERT model based on the LeuT_{Aa} crystal structure [20],

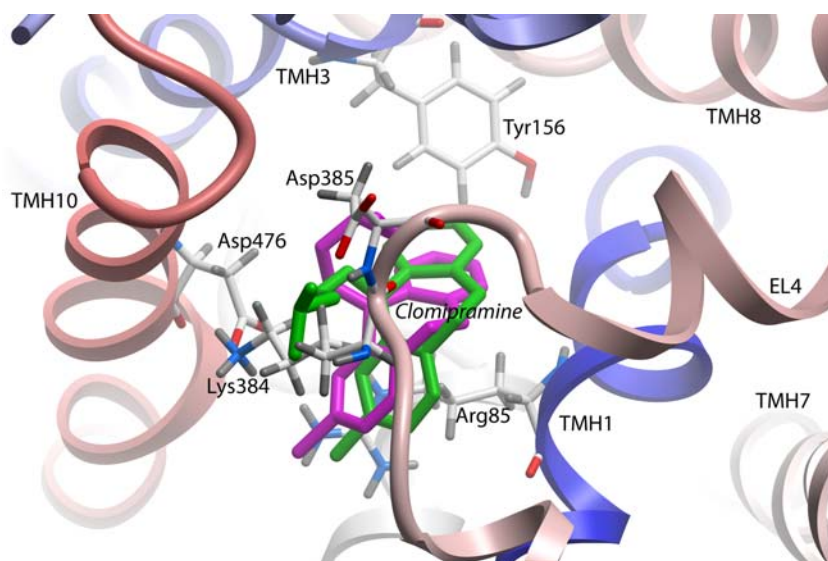


Fig. 7 Clomipramine in DAT binding pocket 2, viewed from extracellular side. *Purple clomipramine* After interactive docking and subsequent docking in flexible DAT, *green clomipramine* superimposed from the crystal structure of a LeuT_{Aa}–clomipramine complex [32]. Amino acids assumed to be part of a clomipramine

binding site according to the LeuT_{Aa}–clomipramine complex [32], and insertion amino acids in EL4 of DAT, Lys384 and Asp385, are displayed as *sticks*. Colour coding: *Red* O, *blue* N, *grey* H, *yellow* C in clomipramine, *white* C in DAT. Colouring of the C α traces of the model is *blue* via *white* to *red* from N-terminal to C-terminal

using a Psi-BLAST (<http://www.ncbi.nlm.nih.gov/BLAST/>) amino acid sequence alignment of LeuT_{Aa}, human glycine transporter (GlyT1b), human GABA transporter (GAT1), human dopamine transporter (DAT), and human SERT [15]. In the present study, we have used a comprehensive sequence alignment of all known prokaryotic and eukaryotic NSS proteins [10] that differs from the previously proposed alignment [20] in TMHs 4, 5 and 9, and in extracellular loops 2, 3, and 4. The present SERT model therefore differs from our previous model in these regions, but not in the areas contributing to the substrate translocation area (TMHs 1, 3, 6 and 8). A multiple sequence alignment highlights evolutionary relationships and increases the probability that corresponding sequence positions are correctly aligned [40].

The EPS calculated from the DAT, SERT and NET models may illustrate the electrostatic aspects of their substrate affinities. These proteins transport positively charged monoamines and are inhibited by cationic drugs. As seen in Figs. 2(a,c), 3(a,c), and 4(a,c), which show the models viewed from the extracellular side, the EPS of the drug recognition site in each model was relatively negative. This clearly indicates that electrostatic forces between the negatively charged binding site and positively charged ligands contribute to ligand recognition and binding to the transporter.

The ICMPocketFinder program identified a possible drug-binding pocket involving TMHs 1, 3, 6 and 8 (binding pocket 1, Table 1) of the DAT, SERT and NET models, in an area corresponding to the substrate-binding pocket of leucine in the LeuT_{Aa} crystal structure [20]. As shown in Fig. 6, binding site 1 includes Asp79 (TMH1), Val152 (TMH3), and Tyr156 (Tyr176 in SERT) (TMH3), previously reported to be important for cocaine binding by site-directed mutagenesis studies [24, 26, 28]. Site-directed mutagenesis data on SERT, DAT and NET also confirm involvement of amino acids in TMH1 [21–25], TMH3 [23, 25–29], TMH6 [30], and TMH8 [30, 31] in the drug-binding area. Figure 5 shows that the two binding pockets are in close proximity and probably slightly overlapping, with Tyr156 (TMH3) and Phe320 (TMH6) participating in both binding pockets.

The location of binding pocket 2, which was identified by ICMPocketFinder, has been confirmed by two X-ray crystal structures of LeuT_{Aa} with TCAs bound in the extracellular-facing cavity [32, 33]. The crystal structure complexes show that TCAs interact with Leu25, Leu29, Arg30, Val33 and Gln34 (TMH1), Tyr107, Tyr108 and Ile111 (TMH3), Phe253 (TMH6), Ala319 and Phe320 (EL4), and Leu400, Asp401 and Asp404 (TMH10) in LeuT_{Aa}. These amino acids correspond to the following DAT residues (Table 2): Leu80, Trp84, Arg85, Tyr88 and Leu89 (TMH1), Phe155, Tyr156 and Ile159 (TMH3),

Phe320 (TMH6), Gly386 and Pro387 (EL4), and Phe472, Thr473 and Asp476 (TMH10). Apparently, TCAs stabilise the extracellular gate of LeuT_{Aa} in closed conformation and inhibit substrate translocation noncompetitively [32, 33]. The orientation of clomipramine after flexible docking (Fig. 7) was similar to that in the LeuT_{Aa} crystal structure complex [32], and interacting DAT residues were in accordance with those in the clomipramine-LeuT_{Aa} X-ray crystal structure complex [32]. The most striking differences between binding pocket 2 of DAT, SERT and NET are in TMH10 (Table 2). The TCA clomipramine is highly selective for SERT over DAT and NET [7]. A possible explanation may be strong interactions between clomipramine and the charged SERT residues Lys490, Glu493 and Glu494 in TMH10. Mutating these SERT residues to alanine may affect clomipramine affinity for SERT. Clomipramine has a low affinity to DAT compared to NET and SERT and, as shown in Table 2, Phe155 in DAT corresponds to tyrosines in NET and SERT. These tyrosines may provide stronger interactions with the nitrogen atom in the tricyclic group of clomipramine than does Phe155 in DAT. A previous docking study of buspirone analogues into a LeuT_{Aa}-based SERT homology model [11] suggested that binding pocket 1 may correspond to a high affinity buspirone binding site, while binding pocket 2 may correspond to a low affinity buspirone binding site.

The DAT, SERT and NET models presented in this study may be considered as working tools for further investigation of their structure and drug interactions. Amino acids in binding pockets 1 and 2 (Tables 1, 2) are obvious candidates for site-directed mutagenesis studies, and the models may be used for docking studies. Interactions seen in drug–target complexes in docking studies can shed light on the intermolecular forces determining the specificities and potencies of drugs. Indeed, structural information about DAT, SERT and NET could potentially aid the structure-aided design of novel neurotransmitter reuptake inhibitors.

Transporter proteins may undergo substantial conformational changes during the transport cycle. Four X-ray crystal structures of the bacterial ABC transporter lipid flippase, MsbA, trapped in different conformations, have shown that large ranges of motion, changing the accessibility of the transporter from a cytoplasmic (inward) facing to an extracellular (outward) facing conformation, may be required for substrate transport [41]. Studies of the bacterial Lac Permease [42] have indicated that widespread cooperative conformational changes, including sliding and tilting motions of the TMHs, may occur during ion and substrate transport. The 12 TMHs may be loosely packed in different conformations associated with transport of substrate molecules. The present DAT, SERT and NET models are based on a closed conformation of LeuT_{Aa} and their

drug recognising conformations, open to the extracellular side, might be slightly different from the closed conformations presented here. The structural flexibility of transporters should be considered when performing docking studies, as insight into structural changes of both the drug and the drug target for adopting an energetically favourable complex (induced-fit) can help predict how a designed drug will fit into a drug target.

References

- Bardo MT (1998) Neuropharmacological mechanisms of drug reward: beyond dopamine in the nucleus accumbens. *Crit Rev Neurobiol* 12:37–67
- Uhl G, Lin Z, Metzger T et al (1998) Dopamine transporter mutants, small molecules, and approaches to cocaine antagonist/dopamine transporter disinhibitor development. *Methods Enzymol* 296:456–465
- Hall FS, Li XF, Sora I et al (2002) Cocaine mechanisms: enhanced cocaine, fluoxetine and nisoxetine place preferences following monoamine transporter deletions. *Neuroscience* 115:153–161
- Uhl GR, Hall FS, Sora I (2002) Cocaine, reward, movement and monoamine transporters. *Mol Psychiatry* 7:21–26
- Schildkraut JJ (1965) The catecholamine hypothesis of affective disorders: a review of supporting evidence. *Am J Psychiatry* 122:509–522
- Manji HK, Duman RS (2001) Impairments of neuroplasticity and cellular resilience in severe mood disorders: implications for the development of novel therapeutics. *Psychopharmacol Bull* 35:5–49
- Tatsumi M, Groshan K, Blakely RD et al (1997) Pharmacological profile of antidepressants and related compounds at human monoamine transporters. *Eur J Pharmacol* 340:249–258
- Barker EL, Blakely RD (1995) Norepinephrine and serotonin transporters: molecular targets of antidepressant drugs. In: Bloom FE, Kupfer DJ (eds) *Psychopharmacology: the fourth generation of progress*. Raven, New York, pp 321–334
- Forrest LR, Tavoulari S, Zhang YW et al (2007) Identification of a chloride ion binding site in Na⁺/Cl⁻-dependent transporters. *Proc Natl Acad Sci USA* 104:12761–12766
- Beuming T, Shi L, Javitch JA et al (2006) A comprehensive structure-based alignment of prokaryotic and eukaryotic neurotransmitter/Na⁺ symporters (NSS) aids in the use of the LeuT structure to probe NSS structure and function. *Mol Pharmacol* 70:1630–1642
- Jaronczyk M, Chilmonczyk Z, Mazurek AP et al (2008) The molecular interactions of bupropion analogues with the serotonin transporter. *Bioorg Med Chem* 16:9283–9294
- Jorgensen AM, Tagmose L, Jorgensen AM et al (2007) Homology modeling of the serotonin transporter: insights into the primary escitalopram-binding site. *Chem Med Chem* 2:815–826
- Ravna AW, Jaronczyk M, Sylte I (2006) A homology model of SERT based on the LeuT(Aa) template. *Bioorg Med Chem Lett* 16:5594–5597
- Ravna AW, Edvardsen O (2001) A putative three-dimensional arrangement of the human serotonin transporter transmembrane helices: a tool to aid experimental studies. *J Mol Graph Model* 20:133–144
- Ravna AW (2006) Three-dimensional models of neurotransmitter transporters and their interactions with cocaine and S-citalopram. *World J Biol Psychiatry* 7:99–109
- Ravna AW, Sylte I, Dahl SG (2003) Molecular model of the neural dopamine transporter. *J Comput Aided Mol Des* 17:367–382
- Ravna AW, Sylte I, Dahl SG (2003) Molecular mechanism of citalopram and cocaine interactions with neurotransmitter transporters. *J Pharmacol Exp Ther* 307:34–41
- Ravna AW, Sylte I, Kristiansen K et al (2006) Putative drug binding conformations of monoamine transporters. *Bioorg Med Chem* 14:666–675
- Xhaard H, Backstrom V, Denessiouk K et al (2008) Coordination of Na⁺ by monoamine ligands in dopamine, norepinephrine, and serotonin transporters. *J Chem Inf Model* 48:1423–1437
- Yamashita A, Singh SK, Kawate T et al (2005) Crystal structure of a bacterial homologue of Na⁺/Cl⁻-dependent neurotransmitter transporters. *Nature* 437:215–223
- Barker EL, Moore KR, Rakhshan F et al (1999) Transmembrane domain I contributes to the permeation pathway for serotonin and ions in the serotonin transporter. *J Neurosci* 19:4705–4717
- Barker EL, Perlman MA, Adkins EM et al (1998) High affinity recognition of serotonin transporter antagonists defined by species-scanning mutagenesis. An aromatic residue in transmembrane domain I dictates species-selective recognition of citalopram and mazindol. *J Biol Chem* 273:19459–19468
- Henry LK, Field JR, Adkins EM et al (2006) Tyr-95 and Ile-172 in transmembrane segments 1 and 3 of human serotonin transporters interact to establish high affinity recognition of antidepressants. *J Biol Chem* 281:2012–2023
- Kitayama S, Shimada S, Xu H et al (1992) Dopamine transporter site-directed mutations differentially alter substrate transport and cocaine binding. *Proc Natl Acad Sci USA* 89:7782–7785
- Lin Z, Wang W, Kopajtic T et al (1999) Dopamine transporter: transmembrane phenylalanine mutations can selectively influence dopamine uptake and cocaine analog recognition. *Mol Pharmacol* 56:434–447
- Chen JG, Sachpatzidis A, Rudnick G (1997) The third transmembrane domain of the serotonin transporter contains residues associated with substrate and cocaine binding. *J Biol Chem* 272:28321–28327
- Larsen MB, Elfving B, Wiborg O (2004) The chicken serotonin transporter discriminates between serotonin-selective reuptake inhibitors. A species-scanning mutagenesis study. *J Biol Chem* 279:42147–42156
- Lee SH, Chang MY, Lee KH et al (2000) Importance of valine at position 152 for the substrate transport and 2β-carbomethoxy-3β-(4-fluorophenyl)tropane binding of dopamine transporter. *Mol Pharmacol* 57:883–889
- Mortensen OV, Kristensen AS, Wiborg O (2001) Species-scanning mutagenesis of the serotonin transporter reveals residues essential in selective, high-affinity recognition of antidepressants. *J Neurochem* 79:237–247
- Roubert C, Cox PJ, Bruss M et al (2001) Determination of residues in the norepinephrine transporter that are critical for tricyclic antidepressant affinity. *J Biol Chem* 276:8254–8260
- Lin Z, Wang W, Uhl GR (2000) Dopamine transporter tryptophan mutants highlight candidate dopamine- and cocaine-selective domains. *Mol Pharmacol* 58:1581–1592
- Singh SK, Yamashita A, Gouaux E (2007) Antidepressant binding site in a bacterial homologue of neurotransmitter transporters. *Nature* 448:952–956
- Zhou Z, Zhen J, Karpowich NK et al (2007) LeuT-desipramine structure reveals how antidepressants block neurotransmitter reuptake. *Science* 317:1390–1393
- Abagyan R, Totrov M, Kuznetsov DN (1994) ICM—a new method for protein modeling and design. Applications to docking

- and structure prediction from the distorted native conformation. *J Comp Chem* 15:488–506
35. Abagyan R, Totrov M (1994) Biased probability Monte Carlo conformational searches and electrostatic calculations for peptides and proteins. *J Mol Biol* 235:983–1002
 36. Laskowski RA, MacArthur MW, Moss DS et al (1993) PRO-CHECK: a program to check the stereochemical quality of protein structures. *J Appl Cryst* 26:283–291
 37. Hoofst RW, Vriend G, Sander C et al (1996) Errors in protein structures. *Nature* 381:272
 38. Colovos C, Yeates TO (1993) Verification of protein structures: patterns of nonbonded atomic interactions. *Protein Sci* 2:1511–1519
 39. Heijne GV (1986) The distribution of positively charged residues in bacterial inner membrane proteins correlates with the trans-membrane topology. *EMBO J* 5:3021–3027
 40. Wieman H, Tondel K, Anderssen E et al (2004) Homology-based modelling of targets for rational drug design. *Mini Rev Med Chem* 4:793–804
 41. Ward A, Reyes CL, Yu J et al (2007) Flexibility in the ABC transporter MsbA: alternating access with a twist. *Proc Natl Acad Sci USA* 104:19005–19010
 42. Kaback HR, Wu J (1997) From membrane to molecule to the third amino acid from the left with a membrane transport protein. *Q Rev Biophys* 30:333–364